Construction and Building Materials 82 (2015) 53–60

Contents lists available at ScienceDirect

Construction and Building Materials

journal homepage: www.elsevier.com/locate/conbuildmat

Application of the logit model for the analysis of asphalt fatigue tests results

Angel Mateos [a,*], Jose Antonio Gómez [b,1], Roberto Hernández [b,1], Yiqiu Tan [c,2], Luis Guillermo Loría Salazar [d,3], Adriana Vargas-Nordcbeck [d,3]

[a] CEDEX Transport Research Center, CEDEX – Ministerio de Fomento, Autovía de Colmenar Viejo km 18.2, 28760 El Goloso, Madrid, Spain
[b] Mexican Institute of Transportation, Km. 12, Carretera Querétaro-Galindo, Sanfandila, 76703 Pedro Escobedo, Querétaro, Mexico
[c] Harbin Institute of Technology, School of Transportation Science and Engineering, Harbin 150090, PR China
[d] University of Costa Rica, National Laboratory of Materials and Structural Models, LanammeUCR, CP-11501-2060 San Jose, Costa Rica

HIGHLIGHTS

- Two models are proposed to reproduce stiffness reduction during asphalt fatigue testing.
- The most suitable model must be selected depending on the level of damage.
- Proposed models significantly improve performance of the models available so far.
- One of the proposed models can reproduce post-failure stiffness reduction.
- One of the models can also reproduce phase angle evolution.

GRAPHICAL ABSTRACT

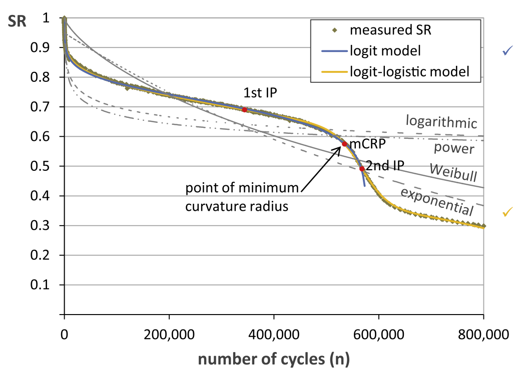

Stiffness Ratio (SR) Models

✓ Logit model can be used to reproduce SR up to the failure phase (mCRP / 2nd IP).

$$SR = SR_0 - \beta \cdot \ln\left(\frac{p^{\gamma}}{1-p^{\gamma}}\right) = SR_0 - \beta \cdot \mathrm{logit}(p^{\gamma})$$

$$p = \frac{n - N_0}{N_L - N_0} \quad \text{(probability of specimen failure)}$$

✓ Logit-logistic model can reproduce SR beyond failure phase.

$$SR = [SR_0 - \beta \cdot \mathrm{logit}(p^{\gamma})] \cdot \left[a + \frac{1-a}{1+e^{b\left(\frac{n}{N1}-1\right)}}\right]$$

Logit-logistic model can also reproduce phase angle evolution.

ARTICLE INFO

Article history:
Received 17 September 2014
Received in revised form 15 January 2015
Accepted 18 February 2015
Available online 6 March 2015

Keywords:
Asphalt mixture
Fatigue testing
Complex modulus
Logit function

ABSTRACT

This paper explores the applicability of the logit function to reproduce the evolution of the stiffness of asphalt specimens during fatigue testing. Three logit-based models are formulated, and they are evaluated on the basis of a comprehensive database. Two of the models are proposed after such evaluation, so the most suitable one must be selected depending on the level of damage the specimen has undergone during testing (up to failure, beyond failure phase). One of these two models was also found to reproduce phase angle evolution. The general conclusion is that proposed models significantly improve performance of other models available so far (exponential, power, logarithmic, and Weibull), and provide an almost perfect fit to experimental data regardless of mixture type and testing procedure and conditions.

1. Introduction

Cracking is considered one of the main distress mechanisms of asphalt pavements. Its importance has been known for decades [1], and its prediction is one of the main goals of the great majority of pavement analytical design approaches, including the AASHTOWare Pavement Mechanistic-Empirical Design software [2]. Either it is initiated at the bottom of the asphalt layer

Abbreviations: SR, stiffness ratio; PR, phase angle ratio.

* Corresponding author. Tel.: +34 91 335 74 59.
E-mail addresses: angel.mateos@cedex.es (A. Mateos), jagomez@imt.mx (J.A. Gómez), rihernan@imt.mx (R. Hernández), tanyiqiu@hit.edu.cn (Y. Tan), luis.loriasalazar@ucr.ac.cr (L.G. Loría Salazar), adriana.vargasnordcbeck@ucr.ac.cr (A. Vargas-Nordcbeck).
1 Tel.: +52 442 216 9777.
2 Tel.: +86 451 86283090.
3 Tel.: +506 2511 2542.

http://dx.doi.org/10.1016/j.conbuildmat.2015.02.029
0950-0618/

(bottom-up) or at the surface (top-down), load-related cracking is the result of asphalt fatigue under traffic loads in combination with environmental effects. Different mechanistic-empirical approaches exist for studying this phenomenon. Most of these approaches are based on laboratory fatigue testing, where an asphalt specimen is subjected to repeated loading until a failure criteria is achieved [3].

The rough output of an asphalt fatigue test is the evolution of the overall stiffness of the specimen *vs* number of cycles (n). Stiffness is characterized in terms of the complex modulus in harmonic-loading tests (typically conducted in bending), while it is characterized in terms of the resilient modulus in pulse-loading tests (typically conducted in indirect-tension) [3]. Complex modulus, E^*, is a complex number whose magnitude, termed dynamic modulus, $|E^*|$, is the ratio of peak cyclic stress to peak cyclic strain under harmonic loading, and whose argument, φ, is referred to as phase angle and is the lag between stress and strain. Resilient modulus (Mr) is the ratio of a pulse-loading peak stress to the strain recovered after the load is retired.

The rough output of asphalt fatigue tests is typically processed for different purposes, with determination of number of cycles to failure (N_f) being the most frequent. A number of failure criteria have been proposed. The simplest criterion establishes N_f as the point where specimen modulus ($|E^*|$ or Mr) is reduced to 50% of its initial value, as it is the case of the European and AASHTO standards for asphalt fatigue testing, EN 12697-24 and AASHTO T 321-07, respectively. Other failure criteria have been proposed based on dissipated energy, a function of $|E^*|\cdot\sin(\varphi)$. For strain-controlled fatigue tests, Hopman et al. [4] and Pronk and Hopman [5] defined energy ratios (ER) that change linearly with the number of cycles until a sharp crack appears in the specimen, thus determining N_f as the point where ER *vs* n deviates from a straight line. Shen et al. [6] used the ratio of dissipated energy change (RDEC), which depends on the slope of the dissipated energy *vs* number of cycles, and they defined N_f as the point where a sharp increase of RDEC takes place. A simplified energy ratio according to Rowe and Bouldin [7], $|E^*|\cdot n$, has been incorporated to ASTM D 7460-10 standard, where N_f is defined as the point where such ratio reaches the maximum value. Processing the rough output of asphalt fatigue tests is also required for modeling purposes [8], and in order to extrapolate fatigue life when the failure criterion is not reached during the test. Different functions have been used with this purpose, which are typically fitted to just part of the available data in a process that involves a high degree of subjectivity [9].

Despite the need of data processing, an appropriate analytical expression is not available for the stiffness reduction curve during fatigue testing and neither for the evolution of the phase angle, which makes data processing time-consuming, cumbersome and, frequently, highly subjective. Several functions have been proposed in order to fit the stiffness reduction curve. The exponential model, $a\cdot\exp(b\cdot n)$, is proposed by AASHTO T 321-07. ASTM D 7460-10 recommends a polynomial function to fit $|E^*|\cdot n$ evolution in order to determine its maximum, while it introduces the Weibull function to extrapolate stiffness reduction when the failure criterion has not been achieved. The use of the Weibull function for predicting stiffness reduction during asphalt fatigue testing was proposed by Tsai et al. [10], who simplified the general expression of this model to the following one: $\ln(-\ln(\mathrm{SR})) = a + b\cdot\ln(n)$, where $\mathrm{SR} = |E^*|/|E^*|_{\mathrm{initial}}$. Prowell et al. [9] used this model to extrapolate fatigue life, and they also evaluated the exponential, power, and logarithmic models, the last two models being $a\cdot n\hat{\ }b$ and $a + b\cdot\ln(n)$, respectively. None of these functions provided acceptable results in all cases, although they concluded the Weibull model appeared to give the most reasonable extrapolation of fatigue test results. The lack of an appropriate function is more evident in the case of the phase angle (φ *vs* n), for which no expression has been proposed so far.

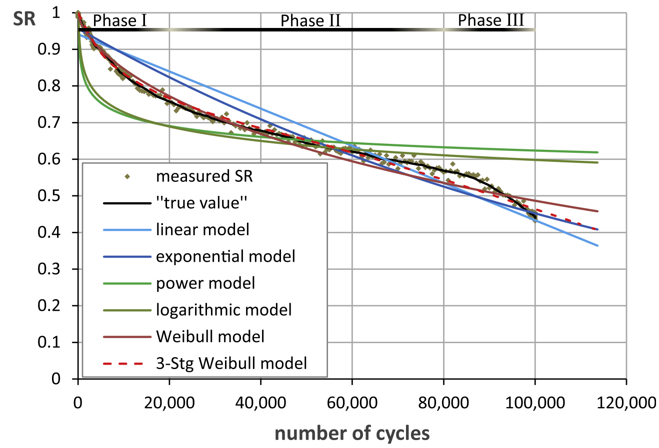

Fig. 1. Example of stiffness ratio evolution during asphalt fatigue testing ($\mathrm{SR} = |E^*|/|E^*|_{\mathrm{initial}}$).

Fig. 1 shows the evolution of stiffness ratio, $|E^*|/|E^*|_{\mathrm{initial}}$, during a typical asphalt fatigue test. Best fits to experimental data (exponential, power, logarithmic, and Weibull models) are also presented in Fig. 1. Three phases can be distinguished in this figure, as reported by Di Benedetto et al. [3]: Phase I, adaptation phase, where a rapid decrease of stiffness takes place (besides asphalt fatigue, heating caused by energy dissipation due to viscoelasticity and probably other reversible phenomena, such as thixotropy, are behind this rapid change); Phase II, quasi-stationary phase, where stiffness changes almost linearly *vs* number of cycles while a network of microcracks is continuously distributed in the material; and finally Phase III, failure phase, where stiffness rate of reduction increases due to coalescence of microcracks to form a sharp crack. This pattern of evolution entails an inflection point, i.e., curvature sign will change during Phase II. This curvature sign change, that has been reported for long time [11], is probably the main reason behind the impossibility of the previous functions (exponential, power, logarithmic, and Weibull) to fit the complete $|E^*|$ *vs* n curve. It can be shown that these four functions result in a curvature that is continuously decreasing in magnitude and always positive. In the best case, they will reproduce half of the complete curve, up to the inflection point, but they never will be able to reproduce the increasing rate of damage accumulation as Phase III approaches. Partial solution to this problem results from piecewise functions, which are defined by multiple sub-functions, each sub-function applying to a certain interval of cycles. This alternative was followed by Tsai et al. [12], who proposed a three-stage Weibull equation with six independent parameters that can be calculated by using a specific software developed by the authors. However, only partial improvement of the goodness of fit is achieved, as reflected in Fig. 1 example.

The Pattern of evolution of measured stiffness ratio in Fig. 1 resembles a sigmoidal function. This shape is actually related to the three phases that take place in fatigue testing, as described above. Consequently, improvement of the goodness of fit could be expected when sigmoidal-type functions are used instead of the constant-curvature-sign functions reported previously. However, this approach has not been evaluated for asphalt fatigue testing.

1.1. Objective

The objective of the research presented herein is to propose and evaluate a sigmoidal-type model that can reproduce the stiffness reduction that takes place during fatigue testing of asphalt mixtures. To propose and evaluate a model to reproduce phase angle evolution is a secondary objective of the research.

1.2. Research approach

Three models are formulated based on sigmoidal functions. The three of them are applicable to the evolution of stiffness ratio during fatigue testing, while the third one is also applicable to the evolution of phase angle (2.1–2.4). The three models are evaluated in terms of their ability to fit actual measured data, which is compared to other models that have been proposed so far (exponential, power, logarithmic, and Weibull). Goodness of fit is quantified in terms of R^2, fitting error, and maximum deviation, which is determined as the maximum difference between model and "true value" of experimental data. This "true value" is a weighted moving average that is calculated by using Excel Forecast function (Fig. 1 example). Excel Forecast fits a linear function to a series of data points (x–y) by using linear regression, and then it uses the fitted linear function to predict y for a particular x value. For each cycle (n_j), the true value of SR is determined as the SR predicted by using Forecast function on the basis of a number of points before and after n_j. Between 4 and 9 points, before and after each experimental value, were used (more points were used as SR rate of reduction was lower). This smoothing approach was found to introduce much less distortion to calculated data than the conventional moving average. The "true value" is also used as a reference in order to estimate test error, s, which was removed from the fitting error, e, in order to determine model error, σ, ($e^2 = s^2 + \sigma^2$). An average of 0.44% was obtained for SR test error throughout all tested specimens, while 0.73% was obtained for phase angle ratio (φ/φ_{ini}). Evaluation of the predictive capability of the models, i.e., ability to predict experimental data beyond the calibration interval, is out of the scope of this paper and it constitutes the objective of an ongoing study.

A comprehensive fatigue tests database was used for this research, comprising 16 asphalt concrete mixtures that were tested in six institutions: CEDEX Transport Research Center (CEDEX), Mexican Institute of Transportation (IMT), University of Costa Rica (UCR), Harbin Institute of Technology (HIT), University of California-Davis (UC), and University of A Coruña (UAC). Fatigue tests included in this research had been conducted within the frame of other research projects. Most tests had been conducted in 4-point bending controlled-strain mode at 20 °C and 10 Hz, according to EN 12697-24 D or AASHTO T 321. Three of the mixtures had been also tested at several temperature and frequency conditions. A total of 28 fatigue tests, comprising 199 tested specimens, were analyzed for this research, which provides an idea of the magnitude of the experimental effort. Most tests had been conducted up to 50% stiffness reduction, while others had been continued until the complete failure of the specimen, in practice, after 80% stiffness reduction (SR = 20%). This experimental design covers a wide range of asphalt mixtures, binder types, and testing conditions, procedures, and devices. Nonetheless, only two of the mixtures had been tested in stress-controlled mode, according to EN 12697-24 E (indirect tension test), which is considered a limitation of the database. Information of the mixtures and testing conditions is presented in Table 1.

Both stiffness and phase angle are handled here in terms of the corresponding ratios, SR and φ/φ_{ini}, after division by the initial measured values. Such values correspond to a specific cycle, n_{ini}, which is defined by the corresponding fatigue standard: AASHTO T 321 uses 50 cycles, while EN 12697-24 uses 100. This cycle is renumbered to 1, and the rest of the cycles are renumbered accordingly. This means that SR = 1 and $\varphi = \varphi_{ini}$ for n = 1. Data before the cycle used to determine initial values, n_{ini}, are not used in the calibration process.

2. Models formulation

2.1. Stiffness reduction model in the arithmetic space

Fig. 1 experimental data are presented in Fig. 2, together with a sigmoidal-type function. The number of cycles in this figure can be conceived as a sigmoidal function of the stiffness ratio, according to Eq. (1), which is based on the logistic curve.

$$n = N_0 + \frac{N_L - N_0}{\left[1 + e^{-\frac{1}{\beta}(SR_0 - SR)}\right]^{1/\gamma}} \tag{1}$$

SR_0, β, N_L, and γ in Eq. (1) are model independent parameters whose meaning is reflected in Fig. 2, while N_0 is a dependent parameter which is formulated in a way, Eq. (2), that SR = 1 for n = 1.

$$N_0 = \frac{-N_L + \left(1 + e^{\frac{1-SR_0}{\beta}}\right)^{1/\gamma}}{-1 + \left(1 + e^{\frac{1-SR_0}{\beta}}\right)^{1/\gamma}} \tag{2}$$

Eq. (1) can be rearranged as shown in Eq. (3). SR can be solved in this equation, resulting the expression in Eq. (4). This equation is based on the logit function, which is the inverse of the sigmoidal logistic function. The logit of a probability α is defined as the logarithm of the odds ratio, $\ln(\alpha/(1-\alpha))$. This model has a number of applications in statistics. It can be noted that the proposed model differs from the logarithmic one in that the number of cycles, n, changes to the odds ratio of the probability of failure raised to γ, i.e., $p^\gamma/(1-p^\gamma)$. The model in Eq. (4) is referred to as logit model hereafter.

$$\left(\frac{n - N_0}{N_L - N_0}\right)^\gamma = p^\gamma = \frac{1}{1 + e^{-\frac{1}{\beta}(SR_0 - SR)}} \tag{3}$$

$$SR = SR_0 - \beta \cdot \ln\left(\frac{p^\gamma}{1 - p^\gamma}\right) = SR_0 - \beta \cdot \text{logit}(p^\gamma) \tag{4}$$

where p is a convenient way to define the probability of failure of the specimen:

$$p = \frac{n - N_0}{N_L - N_0} \tag{5}$$

SR_0, β, N_L, and γ are model independent parameters (Fig. 2), N_0 is a dependent parameter (Eq. (2)).

First and second derivatives of the function are presented in Eqs. (6) and (7), respectively. The number of cycles at the inflection point, where $\ddot{SR} = 0$, can be determined by computing the probability of failure at this critical point from Eq. (8) and then applying Eq. (10). Similarly, the number of cycles corresponding to an arbitrary stiffness ratio can be determined by applying Eqs. (9) and (10).

$$\dot{SR} = \frac{dSR}{dn} = -\frac{\beta \cdot \gamma}{N_L - N_0}\frac{1}{p}\frac{1}{1 - p^\gamma} \tag{6}$$

$$\ddot{SR} = \frac{d^2SR}{dn^2} = -\frac{\dot{SR}}{N_L - N_0}\frac{1}{p}\left(1 - \gamma\frac{p^\gamma}{1 - p^\gamma}\right) \tag{7}$$

probability of failure at the inflection point...

$$p_{IP} = (1 + \gamma)^{-1/\gamma} \tag{8}$$

probability of failure at the stiffness ratio SR_C...

$$p_c = \frac{1}{\left[1 + e^{-\frac{1}{\beta}(SR_0 - SR_C)}\right]^{1/\gamma}} \tag{9}$$

Table 1
Summary of asphalt mixtures and testing conditions.

Mixture id.	Binder cont. (%)	Voids cont. (%)	Binder type[a]	Nmas (mm)	Testing Instit.	Test standard	Temp. (°C)	Freq. (Hz)	No. spec.	SR min.[b] (%)
G20	3.57	5.1	50/70	22	CEDEX	EN 12697-24 D	20	10	9	50
G20+	4.03	4.5	50/70	22	CEDEX	EN 12697-24 D	20	10	8	50
S20	3.78	3.9	50/70	22	CEDEX	EN 12697-24 D	10/20/30	3/10/30	41	50
S20+	4.24	3.3	50/70	22	CEDEX	EN 12697-24 D	20	10	8	50
S20 mod	4.64	4.2	PMB 45/80-65	22	CEDEX	EN 12697-24 D	20	10	10	50
S20 mod+	5.10	3.6	PMB 45/80-65	22	CEDEX	EN 12697-24 D	20	10	8	50
G20b	3.85	6.8	50/70	22	CEDEX	EN 12697-24 D	10/20/30	10	36	40/50
						EN 12697-24 E	20	2[c]	12	50
					UC[d]	AASHTO T 321	10/20	10	10	20
S20 TRC[e]	4.81	4.8	50/70	22	CEDEX	EN 12697-24 D	5/20	10	11	20
G20c	3.70	6.4	50/70	22	UAC	EN 12697-24 E	20	2[c]	2	20
AC20	5.40	6.0	AC-20[f]	19	IMT	AASHTO T 321	20	10	10	50
S12	5.20	6.8	AC-20	19	IMT	AASHTO T 321	20	10	5	20
S20	4.80	6.0	AC-20	19	IMT	AASHTO T 321	20	10	4	20
MDCR-1	6.23	6.3	AC-30	9.5	UCR	AASHTO T 321	20	10	2	50
MDCR-2	5.49	6.5	AC-30	12.5	UCR	AASHTO T 321	20	10	2	50
MDCR-3	4.60	7.5	AC-30	19.0	UCR	AASHTO T 321	10	10	1	20
AC-13C	4.80	4.3	70#	13.2	HIT	AASHTO T 321	5/15	10	20	50

[a] 50/70 is a plain bitumen according to EN 1259. Denomination stands for penetration interval of unaged binder. PMB 45/80-65 is an SBS modified bitumen according to EN 14023. Denomination stands for "Polymer Modified Binder" + penetration interval + ring and ball temperature (°C) of unaged binder. AC-20 and AC-30 are plain bitumens according to ASTM M 226-80. 70# is a plain bitumen according to Chinese standard JTG E20-2011.
[b] Test termination criteria.
[c] 0.1 s haversine loading + 0.4 s rest period.
[d] Specimens were prepared at CEDEX and tested at UC.
[e] Mixture contains 1% (by aggregate mass) recycled tire crumb rubber, dry way.
[f] AC-20 bitumen was modified with SBS polymer.

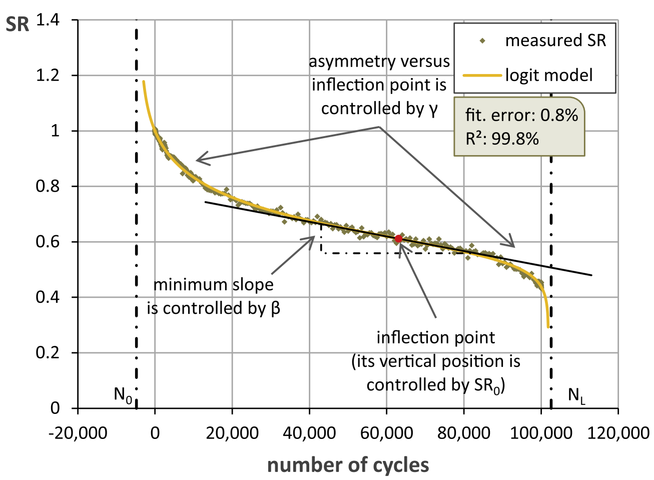

Fig. 2. Stiffness ratio *vs* number of cycles.

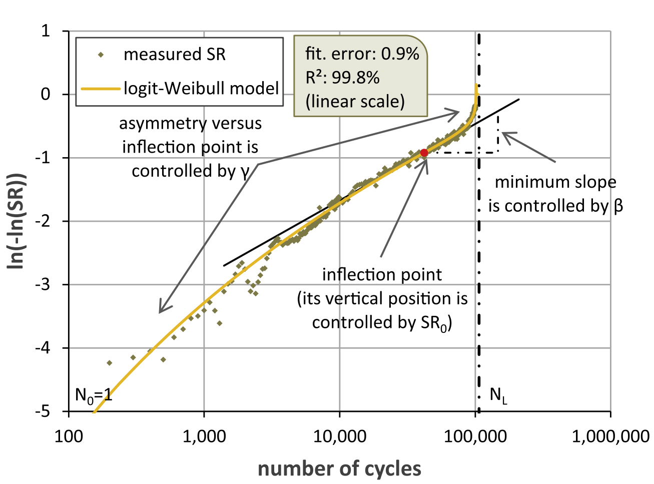

Fig. 3. Stiffness ratio *vs* number of cycles in the Weibull space.

$$n = (1 - p) \cdot N_0 + p \cdot N_L \tag{10}$$

2.2. Stiffness reduction model in the Weibull space

Fig. 1 experimental data can be also represented in the Weibull space, $\ln(-\ln(\mathrm{SR}))$ *vs* $\ln(n)$ (Fig. 3). Data in this figure resemble a sigmoidal function, as they resemble a sigmoidal function in the arithmetic space. The same reasoning that was followed in the arithmetic space can be followed now, and Eq. (11) can be deduced. It can be noted that this model differs from the Weibull one in that the number of cycles, n, changes to the odds ratio of the probability of failure raised to γ, i.e., $p^\gamma/(1-p^\gamma)$. The model in Eq. (11) is referred to as logit–Weibull model hereafter.

$$\begin{aligned}\ln(-\ln(\mathrm{SR})) &= \ln(-\ln(\mathrm{SR}_0)) - \beta \cdot \ln\left(\frac{p^\gamma}{1-p^\gamma}\right) \\ &= \ln(-\ln(\mathrm{SR}_0)) - \beta \cdot \mathrm{logit}(p^\gamma)\end{aligned} \tag{11}$$

where p is a convenient way to define the probability of failure of the specimen:

$$p = \frac{\ln(n)}{\ln(N_L)} \tag{12}$$

SR_0, β, N_L, and γ are model independent parameters (Fig. 3).

First and second derivatives of the function in the Weibull space are presented in Eqs. (13) and (14), respectively. The number of cycles at the inflection point in the Weibull space, where $d^2\ln(-\ln(\mathrm{SR}))/d\ (\ln(n))^2 = 0$, can be determined by computing probability of failure at this critical point from Eq. (15) – the same as in the arithmetic space – and then applying Eq. (17). Similarly, the number of cycles corresponding to an arbitrary stiffness ratio can be determined by applying Eqs. (16) and (17). It can be noted that equations in the Weibull space – Eqs. (11)–(17) – are identical to equations in the arithmetic space – Eqs. (4)–(10) – after changing SR to $\ln(-\ln(\mathrm{SR}))$ and cycle number (n or N_L) to the corresponding logarithm. N_0 term disappears since $N_0 = 1$ in the Weibull space and $\ln(1) = 0$.

$$\frac{d\ \ln(-\ln(\mathrm{SR}))}{d\ \ln(n)} = -\frac{\beta\cdot\gamma}{\ln(N_L)}\frac{1}{p}\frac{1}{1-p^{\gamma}} \tag{13}$$

$$\frac{d^2\ \ln(-\ln(\mathrm{SR}))}{d\ (\ln(n))^2} = -\frac{\frac{d\ \ln(-\ln(\mathrm{SR}))}{d\ \ln(n)}}{\ln(N_L)}\frac{1}{p}\left(1-\gamma\frac{p^{\gamma}}{1-p^{\gamma}}\right) \tag{14}$$

probability of failure at the inflection point...

$$p_{IP} = (1+\gamma)^{-1/\gamma} \tag{15}$$

probability of failure at the stiffness ratio SR_C...

$$p_c = \frac{1}{\left[1+e^{-\frac{1}{\beta}[\ln(-\ln(\mathrm{SR}_0))-\ln(-\ln(\mathrm{SR}_c))]}\right]^{1/\gamma}} \tag{16}$$

$$n = p\cdot\ln(N_L) \tag{17}$$

2.3. Stiffness reduction model after failure phase

Fig. 4 shows the typical evolution of stiffness ratio when a strain-controlled fatigue test is extended until the complete failure (SR → 0). A Phase IV takes place in addition to the three phases reported by Di Benedetto et al. [3]. The rate of change of SR slows down during this fourth phase, probably due to reduction of stress intensity at cracks tips as applied force reduces (strain-controlled test). Rowe and Bouldin [7] refers to this phase as "sample breakdown". This phase cannot be reproduced by the logit model, for which rate of SR reduction continuously increases until the complete failure is reached (SR = 0). A new model, Eq. (18), is proposed for this situation. The new model is the result of the attenuation of the logit function by means of multiplication by a logistic sigmoidal function, as shown in Fig. 4, and it is referred to as logit–logistic model hereafter.

$$\mathrm{SR} = \widehat{\mathrm{SR}}\cdot\left[a+\frac{1-a}{1+e^{b\left(\frac{n}{N1}-1\right)}}\right] \tag{18}$$

where $\widehat{\mathrm{SR}}$ is SR predicted by either logit or logit–Weibull model, Eqs. (4) or (11), respectively, a, b, and $N1$ are model independent parameters (Fig. 4).

The inflection point of the logit function is not reflected in Fig. 4, since it takes place beyond the maximum number of cycles applied during the fatigue test. In fact, the first inflection point of the logit–logistic model is due to the logistic term. This means that this feature of the logit function (its inflection point) is not used in this particular model.

Number of cycles corresponding to 1st and 2nd inflection points (IP) cannot be determined analytically. The same happens for the minimum curvature radius point, which has been referred to as the transition between microcrack formation and the propagation of a macroscopic crack [7]. This point very approximately corresponds to a minimum of the second derivative of SR respect to number of cycles, while inflection points correspond to null second derivative. It is recommended to determine the second derivative of SR numerically, as shown in Eq. (19). The number of cycles corresponding to each of the three characteristics points can be easily determined by using Excel Solver iterative tool.

$$\ddot{\mathrm{SR}} \approx \frac{\mathrm{SR}^{+}-2\cdot\mathrm{SR}+\mathrm{SR}^{-}}{\Delta n^2} \tag{19}$$

where SR^-, SR, and SR^+ are stiffness ratio evaluated at $n-\Delta n$, n, and $n+\Delta n$, respectively, Δn is an increment of cycles (10 cycles have been used in this research).

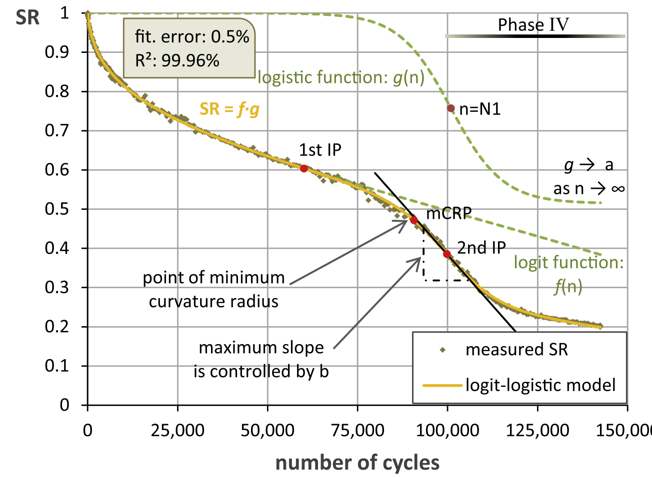

Fig. 4. Stiffness ratio *vs* number of cycles, up to 20% SR (strain-controlled test).

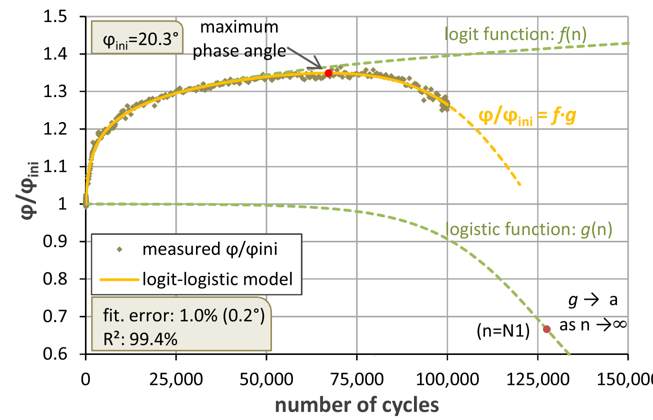

Fig. 5. Phase angle ratio *vs* number of cycles.

2.4. Phase angle evolution model

The logit–logistic model, Eq. (18), was found to be applicable to the evolution of phase angle too. A typical example for such evolution is presented in Fig. 5, which corresponds to the test whose results are presented in Fig. 1. The pattern of evolution observed in Fig. 5 has been described before: phase angle increases as damage accumulates in the asphalt mixture, showing a maximum which has been referred to as the point where microcracks coalesce to form a sharp crack, i.e., transition between micro and macro-cracking [3] [8]. The importance of phase angle in the interpretation of asphalt fatigue tests has been reported for long [13], but no reference was found where an analytical expression for the evolution this variable was proposed. The logit–logistic model can be used to reproduce phase angle evolution. In this case, SR is changed to φ/φ_{ini}, SR_0 parameter is renamed to PR_0, and the logit model has to follow Eq. (4). The expression of the model is presented in Eq. (20).

$$\varphi/\varphi_{ini} = \left[\mathrm{PR}_0-\beta\cdot\ln\left(\frac{p^{\gamma}}{1-p^{\gamma}}\right)\right]\cdot\left[a+\frac{1-a}{1+e^{b\left(\frac{n}{N1}-1\right)}}\right] \tag{20}$$

where p is a convenient way to define the probability of failure of the specimen:

$$p = \frac{n-N_0}{N_L-N_0} \tag{21}$$

Table 2
Goodness of fit of the models.

	[a]	Linear (%)	Exponential (%)	Power (%)	Logarithmic (%)	Weibull (%)	Logit, Eq. (4) (%)	Logit (ϒ = 1), Eq. (4) (%)	Logit–Weibull, Eq. (11) (%)	Logit–Weibull (ϒ = 1), Eq. (11) (%)	Logit–logistic, Eqs. (18) and (4) (%)	Logit–logistic (ϒ = 1), Eqs. (18) and (4) (%)	Logit–Weibull–logistic, Eqs. (18) and (11) (%)	Logit–Weibull–logistic (ϒ = 1), Eqs. (18) and (11) (%)
SR min. 50% (19 tests)	R^2	79.5	86.9	82.1	88.0	98.5	99.7	99.6	99.7	99.4				
	σ	5.5	4.6	5.7	4.5	1.4	0.4	0.6	0.5	0.8				
	δm	11.8	10.2	12.6	10.5	3.7	1.2	1.6	1.4	2.3				
SR min. 40%[b] (8 tests)	R^2	90.8	92.8	86.3	90.5	98.8	99.9	99.7	99.9	99.5				
	σ	5.4	4.6	7.1	5.8	1.9	0.5	0.8	0.5	1.1				
	δm	10.7	9.3	19.2	16.1	6.9	1.5	2.2	1.5	4.2				
SR min. 20% (7 tests)	R^2	89.4	91.2	67.6	76.7	95.7					99.9	99.8	99.9	99.7
	σ	5.4	5.0	10.8	8.9	3.6					0.3	0.6	0.4	0.8
	δm	12.7	12.9	30.7	26.0	12.9					1.0	1.5	1.6	2.5

[a] σ is model error. δm is maximum deviation from the "true value" of the data. First 100 cycles are not considered in the calculation of δm of power and logarithmic models.
[b] This group includes one test conducted until 40% SR and also the tests conducted until SR = 20% but using only data corresponding to SR over 40% (Table 1).

PR_0, β, N_L, and γ are independent parameters of the logit part of the equation, N_0 is a dependent parameter (Eq. (2), after changing SR_0 to PR_0), a, b, and $N1$ are independent parameters of the logistic part of the equation (Fig. 5).

3. Models evaluation

3.1. Evaluation of the stiffness reduction models

Table 2 shows the goodness of fit of the models. The first conclusion that can be deduced is the excellent agreement achieved by the three models proposed in this paper. Logit and logit–Weibull models were used for tests conducted until 50% and 40% SR, while the logit–logistic model according to Eq. (18) was used for tests conducted until the complete failure of the specimen (SR = 20%). The average error of the proposed models was between 0.3% and 0.5%, which is comparable to test error. Performance of the logit model was slightly better than performance the logit–Weibull model, especially when used together with the logistic term for 20%-SR data. Besides, the logit model provided an excellent fit even without considering γ asymmetry parameter, i.e., making $\gamma = 1$. Strong asymmetry of the experimental data in the Weibull space, as reflected in Fig. 3 example, is the reason behind the relatively poor results of the logit–Weibull model when γ parameter was set to 1. Performance of the Weibull model was very good compared to linear, exponential, power, and logarithmic models, but it was still far from the logit and logit–logistic models, especially for tests conducted up to 40% and 20% SR. This can be appreciated in Fig. 6, which shows maximum deviation of the models with respect to the "true value" of the experimental data.

Figs. 7 and 8 show representative examples of the goodness of fit that was achieved by the logit model for tests conducted until 50% and 40% SR, respectively (model errors in these figures are similar to average values in Table 2). An excellent agreement can be appreciated in these figures. The same is applicable to the logit–Weibull model. Problems with these two models only appeared when fitting data beyond the minimum curvature radius point. After this point, as explained above, these two models result in a curvature that continuously increases (in absolute value) until complete failure of the specimen, so they cannot reproduce the reducing rate of damage accumulation that takes place during Phase IV of strain-controlled fatigue tests. The logit–logistic model should be used in these cases, regardless of the minimum SR that is reached during testing. Fig. 9 shows a representative example of

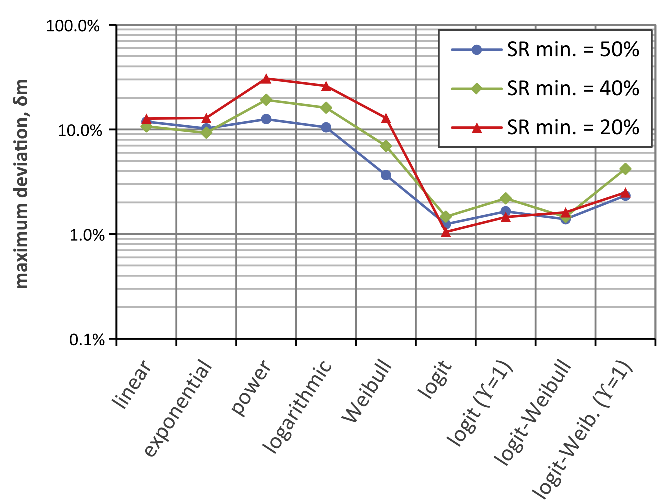

note: the logistic term, according to Eq. (18), is added to logit and logit-Weibull models for 20% SR min.

Fig. 6. Maximum deviation of the models from the "true value" of the data.

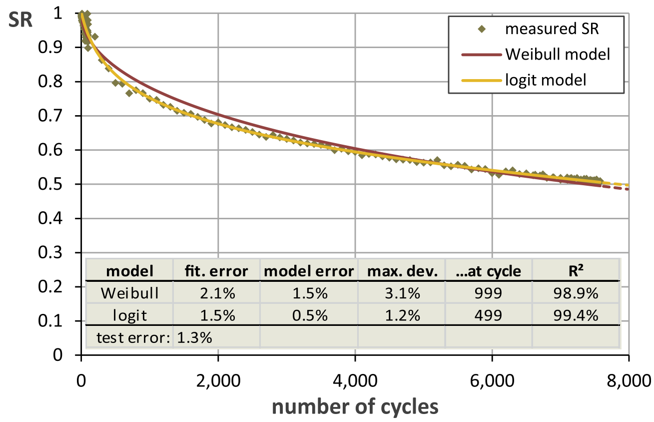

Fig. 7. Example of test conducted up to 50% SR; G20b (CEDEX), EN 12697 D, 30 °C and 10 Hz, 450 $\mu\varepsilon$.

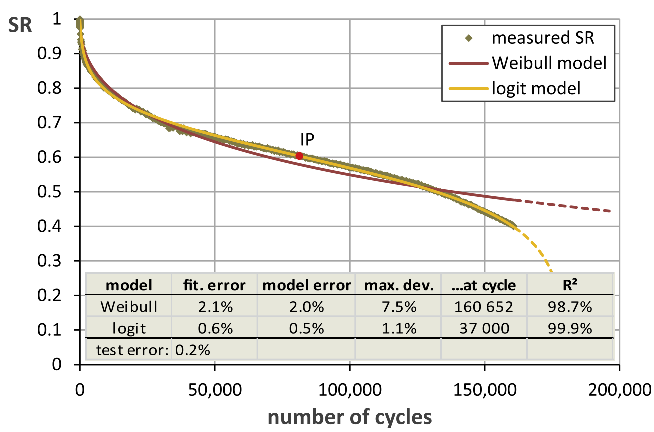

Fig. 8. Example of test conducted up to 40% SR; G20b (CEDEX), EN 12697 D, 20 °C and 10 Hz, 125 $\mu\varepsilon$.

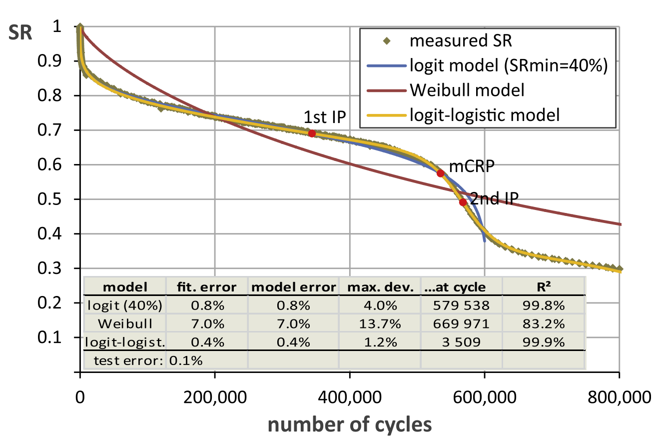

Fig. 9. Example of test conducted up to 20% SR; S12 (IMT), AASHTO T 321, 20 °C and 10 Hz, 300 $\mu\varepsilon$.

the goodness of fit that was achieved by the logit–logistic model for tests conducted until 20% SR. The general conclusion is that proposed models errors were more related to test error and irregularities (sudden changes in SR due specimen fixing problems, aggregate readjustment, etc.) rather than to the actual shape of the experimental data.

As explained above, the logit–logistic model has to be used for tests where post-failure data are available, as the example shown in Fig. 9. This situation does not apply to stress-controlled tests, where rate of damage accumulation continuously increases until the complete failure of the specimen. Only two tests of the database were conducted in stress-controlled mode, and only for one of them the test was continued until 20% SR (G20c mixture, Table 1). Both logit and logit–Weibull models, without including the logistic term, provided an excellent fit for this test, with average maximum deviation and model error of 1.1% and 0.2%, respectively. This seems to indicate that the applicability of the proposed models could be even better for stress-controlled data, although this result should be considered with caution since it is based on only two test specimens.

Both logit and logit–Weibull models have four independent parameters, which is considered the minimum number to reproduce the stiffness reduction when fatigue tests are conducted until Phase III (failure phase). Conceptually, three parameters are required to determine n, SR, and SR slope at the inflection point and one additional parameter is required to define the asymmetry of the data with respect to the inflection point (Fig. 8). When post-failure data are available (Phase IV), three additional parameters are required to determine n, SR, and SR slope at the second inflection point, and at least one more to determine the long-term (as $n \to \infty$) evolution of SR. This means at least eight parameters (Fig. 9), which is higher than the number of independent parameters of the logit–logistic model. Actually, both long-term evolution and vertical position of the second inflection point are controlled by the parameter "a" of the logistic term. Unfortunately, the γ parameter of this model does not control the asymmetry of the function with respect to the first inflection point, but only the shape of the modulus descent during adaptation Phase I.

Models parameters were determined by using Excel Solver iterative tool (GRG nonlinear option), with the aim of minimizing fitting error. Convergence was achieved for the logit model in all cases starting with the seed values $SR_0 = 0.5$, $\beta = 0.1$, $\gamma = 1$, and $N_L = 1.2{\cdot}N_{max.}$ ($N_{max.}$ is maximum number of test cycles). For the logit–Weibull model, convergence was achieved in almost all cases with the seed values $SR_0 = 0.8$, $\beta = 0.4$, $\gamma = 1$, and $N_L = 1.2{\cdot}N_{max}$. Convergence problems resulted for 4 specimens where intermediate solutions of the iterative process gave $SR_0 > 1$ and, consequently, $\ln(-\ln(SR_0))$ produced an error. This problem could be overcome by forcing $SR_0 = 0.99$ at first, leaving β, γ, and N_L as fitting parameters, and then repeating the iterative process – with all parameters – using the output of the first step as seed values. Parameters of the logit–logistic model were determined in two steps: the model was first calibrated without the logistic term (forcing $a = 1$) and then the iterative process was repeated – with all parameters – using the output of the first step as seed values for SR_0, β, γ, and N_L, and using 0.5 and 2 as seed values for a and b, respectively. $N1$ seed value had to be visually estimated.

3.2. Evaluation of the phase angle evolution model

The evolution of phase angle during fatigue tests was reproduced by using the logit–logistic model, according to Eq. (20), regardless of the minimum SR. The logistic term is necessary in order to reproduce the descendent φ during specimen failure. An excellent agreement was obtained, with an average R^2 of 98.3%, an average model error (σ) of 1.0%, and an average maximum deviation (δm) of 2.5%. In terms of sexagesimal degrees, σ was 0.2° and δm was 0.4°. Very similar results ($\sigma = 1.1\%$ and $\delta m = 2.8\%$) were obtained when γ asymmetry parameter was set to 1. Besides, no significant differences (p value = 0.298) were obtained between error of tests conducted until 40/50% SR and error of tests conducted until 20% SR. The example of phase angle ratio evolution in Fig. 5 is representative of the average goodness of fit achieved by the logit–logistic model. This model presented difficulties only for some specimens where a very rapid decrease of phase angle took place at the end of the test. In the rest of the cases, fitting error was more related to test error and irregularities rather than to the actual pattern of evolution of experimental data. The same conclusion was obtained for SR proposed models, although test irregularities affected φ much more than $|E^*|$.

4. Conclusions

Three logit-based models have been formulated in order to reproduce stiffness ratio evolution during asphalt fatigue testing (SR *vs* n), and they have been evaluated on the basis of a comprehensive experimental database. Based on this evaluation, two models are proposed which significantly improve performance of other models available so far (exponential, power, logarithmic, and Weibull). Proposed models provide an almost perfect fit to experimental data regardless of mixture type and testing procedure and conditions. The most suitable model should be selected depending on the level of damage the specimen has undergone during testing:

- When fatigue tests are conducted up to the failure phase, a four independent parameters model is proposed whose equation is as simple as $SR = SR_0 - \beta \cdot \mathrm{logit}(p^{\gamma})$, where p is probability of specimen failure, $p = (n - N_0)/(N_L - N_0)$. This model (termed "logit" in this study) provided average R^2, model error, and maximum deviation with respect to experimental data of 99.8%, 0.5%, and 1.4%, respectively, for tests conducted up to 50% or 40% stiffness ratio.
- When strain-controlled fatigue tests are conducted beyond the failure phase, stiffness ratio rate of reduction slows down, and a seven independent parameters model is proposed. This model (termed "logit–logistic" in this study) is the result of the attenuation of the logit function by means of multiplication by a logistic sigmoidal function. It provided average R^2, model error, and maximum deviation of 99.9%, 0.3%, and 1.0%, respectively, for tests conducted up to 20% stiffness ratio.

Another advantage of the proposed models is the excellent convergence when parameters are determined by using Excel Solver iterative tool. It is shown in this paper that the minimum number of independent parameters that are required to reproduce SR evolution is four or eight, depending on whether the test is conducted up to or beyond the failure phase, i.e., depending on whether one or two inflection points are present in experimental data.

The logit–logistic model was found to be also applicable to reproduce the evolution of phase angle ratio (PR *vs* n), regardless of the damage the specimen has undergone during testing. Average R^2, model error, and maximum deviation were 98.3%, 1.0%, and 2.5%, respectively.

The general conclusion, for both SR and PR models, is that fitting errors were more related to test error and irregularities rather than to the actual pattern of evolution of experimental data.

Acknowledgements

Authors would like to express their gratitude for the important laboratory effort behind this study. Workers who made it possible are sincerely acknowledged and recognized.

References

[1] European Commission. COST 333 "Development of New Bituminous Pavement Design Method". Final Report of the Action. European Commission, Directorate General Transport, Brussels; 1999.
[2] American Association of State Highway and Transportation Officials (AASHTO). Mechanistic-Empirical Pavement Design Guide: A Manual of Practice. Washington, D.C.: AASHTO; 2008.
[3] Di Benedetto H, De La Roche C, Baaj H, Pronk A, Lundström R. Fatigue of bituminous mixtures. Mater Struct 2004;37(3):202–16. http://dx.doi.org/10.1007/BF02481620.
[4] Hopman PC, Kunst PAJC, Pronk AC. A renewed interpretation method for fatigue measurements, verification of Miner's Rule. In: 4th Eurobitume Symposium in Madrid, vol. 1; 1989, p. 557–561.
[5] Pronk AC, Hopman PC. Energy dissipation: The leading factor of fatigue, highway research: sharing the benefits. In: Proceedings of the Conference, the United States Strategic Highway Research Program, London; 1990. p. 225–237.
[6] Shen S, Airey GD, Carpenter SH, Huang H. A dissipated energy approach to fatigue evaluation. Road Mate Pavement Des 2006;7(1):47–69.
[7] Rowe GM, Bouldin MG. Improved techniques to evaluate the fatigue resistance of asphaltic mixtures. In: Proceedings of 2nd Eurasphalt and Eurobitume Congress, vol. 1, Barcelona; 2000. p. 754–763.
[8] Tapsoba N, Sauzéat C, Di Benedetto H. Analysis of fatigue test for bituminous mixtures. J Mater Civ Eng 2013;25(6):701–10. http://dx.doi.org/10.1061/(ASCE)MT.1943-5533.0000636.
[9] Prowell B, Brown E, Anderson RM, Swamy JSDAK, Von Quintus H, Shen S, Maghsoodloo S. Validating the fatigue endurance limit for hot mix asphalt. NCHRP Report 646. Transportation Research Board, National Academies of Sciences; 2010.
[10] Tsai BW, Harvey JT, Monismith CL. High temperature fatigue and fatigue damage process of aggregate-asphalt mixes. J Assoc Asphalt Paving Technol 2002;71:345–85.
[11] Rowe GM. Performance of asphalt mixtures in the trapezoidal fatigue test. J Assoc Asphalt Paving Technol 1993;62. 344–344.
[12] Tsai BW, Harvey JT, Monismith CL. Using the three-stage Weibull equation and tree-based model to characterize the mix fatigue damage process. Transp Res Rec: J Transp Res Board 2005;1929(1):227–37.
[13] Reese R. Properties of aged asphalt binder related to asphalt concrete fatigue life. J Assoc Asphalt Paving Technol 1997;66:604–32.